Diffusion tensor imaging of cingulum fibers in mild cognitive impairment and Alzheimer disease

Y. Zhang, MD; N. Schuff, PhD; G.-H. Jahng, PhD; W. Bayne, BS; S. Mori, PhD; L. Schad, PhD; S. Mueller, MD; A.-T. Du, MD; J.H. Kramer, PsyD; K. Yaffe, MD; H. Chui, MD; W.J. Jagust, MD; B.L. Miller, MD; and M.W. Weiner, MD

Abstract—*Background:* Neuroimaging in mild cognitive impairment (MCI) and Alzheimer disease (AD) generally shows medial temporal lobe atrophy and diminished glucose metabolism and cerebral blood flow in the posterior cingulate gyrus. However, it is unclear whether these abnormalities also impact the cingulum fibers, which connect the medial temporal lobe and the posterior cingulate regions. *Objective:* To use diffusion tensor imaging (DTI), by measuring fractional anisotropy (FA), to test 1) if MCI and AD are associated with DTI abnormalities in the parahippocampal and posterior cingulate regions of the cingulum fibers; 2) if white matter abnormalities extend to the neocortical fiber connections in the corpus callosum (CC); 3) if DTI improves accuracy to separate AD and MCI from healthy aging vs structural MRI. *Methods:* DTI and structural MRI were preformed on 17 patients with AD, 17 with MCI, and 18 cognitively normal (CN) subjects. *Results:* FA of the cingulum fibers was significantly reduced in MCI, and even more in AD. FA was also significantly reduced in the splenium of the CC in AD, but not in MCI. Adding DTI to hippocampal volume significantly improved the accuracy to separate MCI and AD from CN. *Conclusion:* Assessment of the cingulum fibers using diffusion tensor imaging may aid early diagnosis of Alzheimer disease.

NEUROLOGY 2007;68:13–19

Structural MRI studies found prominent volume losses in the entorhinal cortex and hippocampus in mild cognitive impairment (MCI)[1-3] and Alzheimer disease (AD)[4-6] while PET and SPECT studies found functional reductions primarily in the posterior cingulate.[7-12] The regional dissociation between structural and functional abnormalities may be due to reduced neuronal traffic between medial temporal lobe and posterior cingulate. Thus the cingulum fibers which connect the medial temporal lobe and the posterior cingulate[13,14] may be involved in early AD. In late AD, as the disease spreads to the cortex,[15] neocortical connections, such as corpus callosum (CC), may also be afflicted.

Diffusion tensor imaging (DTI) is used to detect degradation of white matter fiber bundles,[16-18] by measuring fractional anisotropy (FA) and mean diffusivity (D).[19] Several DTI studies of AD found abnormal FA and D in posterior cingulate,[20-22] temporal, parietal lobes,[23,24] and CC.[22,25-27] However, the regional patterns of abnormal DTI values were not consistent. Moreover, previous DTI assessments were limited to the posterior cingulate, while fiber extensions to medial temporal lobe were not evaluated. Furthermore, the diagnostic utility of DTI for MCI and AD as compared to conventional hippocampal volumetry has not been determined.

The main goals of this study were 1) to test if abnormal DTI values along the cingulum fibers are associated with MCI and AD pathology; and 2) to test if DTI measures improve the accuracy to separate MCI and AD from healthy aging over hippocampal volume loss.

Methods. *Population.* Seventeen subjects diagnosed with MCI (age 73.1 ± 7.4 years; 9 men, 8 women), 17 patients

Editorial, see page 9

From VA Medical Center and UC San Francisco (Y.Z., N.S., G.-H.J., W.B., S. Mueller, A.-T.D., M.W.W.), CA; Johns Hopkins University (S. Mori), Baltimore, MD; German Cancer Research Institute (L.S.), Heidelberg, Germany; UC San Francisco (J.H.K., K.Y., B.L.M.), CA; University of Southern California (H.C.), Los Angeles; and Lawrence Berkeley National Laboratory and UC Berkeley (W.J.J.), CA.

Supported in part by NIH/NIA RO1 AG10897, NIH/NIA PO1 AG012435, NIH/NIA P50 AG23501, and DOD DAMD17-01-1-0764.

Disclosure: The authors report no conflicts of interest.

Received March 15, 2006. Accepted in final form September 1, 2006.

Address correspondence and reprint requests to Dr. Yu Zhang, MR Unit (114M), VA Medical Center, 4150, Clement Street, San Francisco, CA 94121; e-mail: Yu.Zhang@ucsf.edu

Copyright © 2007 by AAN Enterprises, Inc.

Copyright © by AAN Enterprises, Inc. Unauthorized reproduction of this article is prohibited.

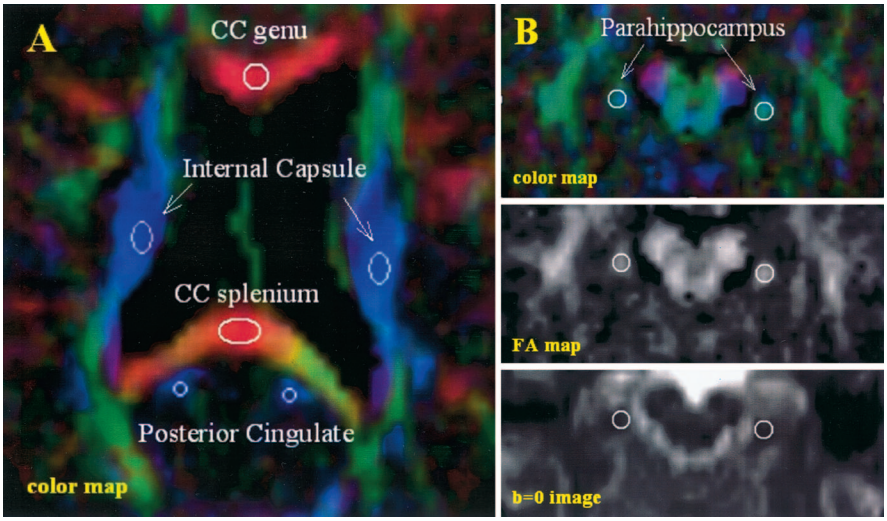

Figure 1. Illustration of the region of interest (ROI) selection: (A) ROIs at bilateral posterior cingulate, internal capsule, and corpus callosum (genu and splenium); (B) the ROIs at the parahippocampal region, and same regions overplayed on the FA and b = 0 images.

diagnosed with AD (age 77.1 ± 8.8 years; 8 men, 9 women), and 18 cognitive normal (CN) subjects (71.6 ± 9.2 years; 10 men, 8 women) were included in this observational study. Patients with AD and MCI were referred from the University of California at San Francisco (UCSF) and Davis (UCD) AD treatment centers, and CN subjects were recruited from populations, between July 2002 and April 2005. All participants underwent a series of neurologic tests and a battery of neuropsychological assessments, which included the Mini-Mental State Examination (MMSE)[28] and the Clinical Dementia Rating Scale (CDR)[29] at UCSF. MCI was determined according to either the Petersen criteria[30] or the criteria established by the AD Cooperative Study (ADCS).[31] Three of the MCI subjects were diagnosed with amnesic MCI, according to Petersen criteria, while the remaining MCI subjects presented a broader range of cognitive impairments. All patients with AD fulfilled the National Institute of Neurologic and Communicative Disorders and Stoke and AD and Related Disorders Association (NINCDS-ADRDA) criteria[32] for probable AD. The CN subjects had no history of a psychiatric or neuropsychological disease, major heart disease, diabetes, cardiovascular disease, epilepsy, or head trauma, and furthermore, scored within the normal range on all cognitive tests. A neuroradiologist reviewed the MR images from each subject to confirm absence of major neuropathologies, such as tumors and infarctions. Furthermore, subjects with extensive white matter lesions (WML) involving fibers of interest were not included in this study. In general, however, subjects with WML not extending into the regions of interest were included in this study. An experienced radiologist reviewed all T1, T2-weighted, and proton density images to determine severity of WML. In addition, the severity of WML was classified as mild (score 1), moderate (score 2), or severe (score 3), according to Scheltens' rating scale.[33] All subjects or their legal guardians gave written informed consent before participation in the study, which was approved by the committees of Human Research at UCSF and the VA Medical Center.

MRI acquisition. All examinations were preformed on a 1.5 Tesla MR system (Siemens Vision System, Germany), using a standard head coil. Structural MRI included volumetric T1-weighted magnetization-prepared rapid acquisition gradient-echo (MPRAGE) images (repetition time [TR]/echo time [TE]/inversion time [TI] = 10/7/300 msec, flip angle = 15°, 1 × 1 × 1.4 mm^3 resolution) for hippocampal tracing and tissue segmentation and multi-slice proton density and T2-weighted images based on a dual-echo sequence (TR/TE1/TE2 = 5000/20/80 msec, 1.25 × 1 mm^2 in-plane resolution, 3 mm slice thickness, without gap between slices) for measuring total intracranial volume and the extent of white matter hyperintensity. DTI was performed using an inversion-prepared double refocused single-shot echoplanar imaging (EPI) sequence[34] (TR/TE/TI = 6000/100/2000 msec; 2.34 × 2.34 in-plane resolution, 19 contiguous slices, each 5 mm thick), with bipolar diffusion sensitizing gradients of b = 1000 s/mm^2 applied along six directions. Additional spin-echo EPI scans without diffusion gradients (b = 0 image) were also acquired for normalizing diffusion measurements. Inversion recovery reduced contributions from CSF to the diffusion signal and double-refocusing RF pulses with bipolar gradients reduced geometric distortions in DTI due to eddy currents.

Hippocampal volumetry. Hippocampal boundaries were traced semi-automatically on MPRAGE images using a high dimensional brain-warping algorithm (Medtronic Surgical Navigation Technologies, Louisville, CO). We previously validated this method in comparison to manual tracing hippocampus in patients with AD and healthy subjects.[35] Manual and semi-automated volume measurements of the hippocampus generally correlated better than 90%. Furthermore, hippocampal boundaries from semi-automated tracing were visually reviewed scan by scan and manually corrected if misregistrations occurred, thus further diminishing differences between manual and automated measurements. Hippocampal volumes were furthermore normalized to total intracranial volumes (TIV) to account for variations of head size.

DTI data postprocessing. The DTI images were processed offline. DTIstudioV2 software[36] (Johns Hopkins University, Baltimore, MD) was used to create FA, D, and color-coded directionality maps of diffusion, that were overlaid on each other. The color-coded directional maps (red: left-to-right direction, green: anterior-to-posterior direction, blue: superior-to-interior direction) provided easy visualization of the white matter fiber tracts. Elliptical regions of interest (ROI) were drawn based on the identification of white matter tracts on the color-coded maps.[21,25] A total of four pairs of ROIs were placed on axial slices to select the following white matter regions (figure 1): 1) bilateral parahippocampal regions on the medial temporal portion of the cingulum fibers at a slice level where the full view of the hippocampal formation could be identified; 2) bilateral posterior cingulate regions, at the middle level of the dorsal curve of the cingulum fibers; 3) genu and splenium ROIs at the center of anterior and posterior CC; 4) for reference, bilateral regions at the posterior limb of internal capsule, where sensorimotor fiber converge and no degradations related to MCI or AD are expected. FA and D values within each ROI were averaged. ROIs were placed to maximally encompass each white matter fiber tract, and had generally an in-plane size of 4 × 4 mm^2 to 6 × 9 mm^2, with 5 mm slice thickness. The ROI sizes were kept fixed for all subjects. To account for potential variation of fiber thickness with head size, TIV was included as a covariate in the group analysis of DTI data. An experienced radiologist (Y.Z.), blinded to subject information including diagnosis, performed the ROI drawings. To determine reliability of the ROI measurements, the same rater repeated ROI drawings on 12 randomly selected subjects, blinded to the previous readings. Reliability, expressed as an intraclass correlation coefficient, was 0.96 for the DTI measurements.

Statistics. Variations of FA and D of each ROI were analyzed separately as a linear function of diagnosis with adjustments for age, sex, and TIV. A similar linear model was used to analyze

Copyright © by AAN Enterprises, Inc. Unauthorized reproduction of this article is prohibited.

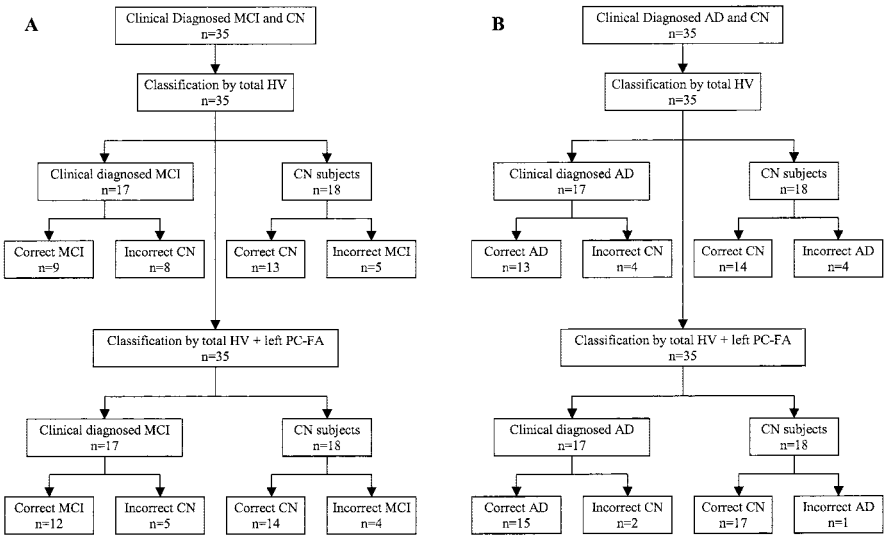

Figure 2. Classification of mild cognitive impairment and cognitively normal (CN) (A), Alzheimer disease and CN (B) by using total hippocampal volume (total HV) alone vs using total HV + left posterior cingulate fractional anisotropy (FA) (left PC-FA).

variations of hippocampal volumes. To determine if diagnosis and age added explanatory power and were therefore needed in the models, three nested models were fitted by maximum likelihood: the first (base) model included only the covariates, while diagnosis and a diagnosis × age interaction were sequentially added in the second and third model, respectively. The resulting fits were compared sequentially via *F*-tests to determine if diagnosis or diagnosis × age added explanatory power ($p < 0.05$) to the base model. To estimate the magnitude of group effects, effect sizes were calculated according to the following:

$$Effect\ \ Size = \frac{Mean_1 - Mean_2}{\sqrt{\frac{(n_1 - 1)Std_1^2 + (n_2 - 1)Std_2^2}{(n_1 - 1) + (n_2 - 1)}}}$$

where $Mean_{1/2}$ and $Std_{1/2}$ represent mean and SD, respectively, of measures in Groups 1 and 2, and $n_{1/2}$ are the number of subjects in Group 1 and 2. The powers of DTI and hippocampal volume measures to correctly classify CN, MCI, and AD were estimated based on logistic regressions and sensitivity and specificity of the classifications were expressed in terms of a receiver operator characteristics analysis as area under the curve (AUC). The logistic regressions were further adapted to a random leave-one-out procedure for cross-validation of the classifications. Finally, AUCs from cross-validations were compared using Wilcoxon signed rank tests. The statistical computations were performed using Splus 6.3 (Insightful Inc., Seattle, WA). The significance level was $\alpha < 0.05$ in all tests.

Results. All the subjects had satisfactory MRI quality and their data were included in the statistical analyses (figure 2). Demographics and clinical information of the subjects are summarized in table 1. There was no difference between the groups in age ($p = 0.14$, ANOVA), sex ($\chi^2 = 0.08$, $p > 0.7$), or years of education ($p = 0.25$, ANOVA). Furthermore, WML severity, which is also listed in table 1, and broken down into mild:moderate:severe, was similar between the groups ($p = 0.82$). As expected, patients with AD had markedly lower MMSE scores than

Table 1 *Demographics*

	CN	MCI	AD
Number	18	17	17
Age, y, mean ± SD	71.6 ± 9.2	73.1 ± 7.4	77.1 ± 8.8
M:F	10:8	9:8	8:9
Education, y, mean ± SD	15.5 ± 2.7	15.8 ± 2.6	14.2 ± 3.6
WML, mild:moderate:severe	13:0:5	9:5:3	11:4:2
MMSE, mean ± SD	29.5 ± 0.8	27.9 ± 2.0	22.1 ± 4.0
CDR, mean ± SD	0.0 ± 0.0	0.5 ± 0.0	1.0 ± 0.4

CN = cognitive normal; MCI = mild cognitive impairment; AD = Alzheimer disease; WML = white matter lesions; MMSE = Mini-Mental State Examination; CDR = Clinical Dementia Rating Scale.

Table 2 *Group effects of diagnosis on fractional anisotropy*

Dependent variable	Coefficients value	SE	*p* Value	Effect size
AD vs CN				
Left PH	−0.27	0.08	0.002	−1.14
Right PH	−0.18	0.09	0.04	−0.72
Left PC	−0.42	0.08	<0.0001	−1.76
Right PC	−0.28	0.07	0.003	−1.36
sCC	−0.37	0.11	0.003	−1.22
gCC	−0.11	0.12	0.39	−0.59
MCI vs CN				
Left PH	−0.24	0.09	0.01	−0.96
Right PH	−0.18	0.07	0.02	−0.76
Left PC	−0.23	0.07	0.003	−1.07
Right PC	−0.04	0.07	0.59	−0.14
sCC	−0.12	0.07	0.11	−0.5
gCC	−0.07	0.13	0.6	−0.26
AD vs MCI				
Left PH	−0.03	0.09	0.69	−0.1
Right PH	0.03	0.09	0.79	−0.06
Left PC	−0.15	0.09	0.12	−0.6
Right PC	−0.24	0.08	0.004	−1.09
sCC	−0.29	0.11	0.01	−0.89
gCC	−0.03	0.14	0.81	−0.29

AD = Alzheimer disease; CN = cognitive normal; PH = parahippocampus; PC = posterior cingulate; sCC = splenium and gCC = genu of the corpus callosum; MCI = mild cognitive impairment.

Copyright © by AAN Enterprises, Inc. Unauthorized reproduction of this article is prohibited.

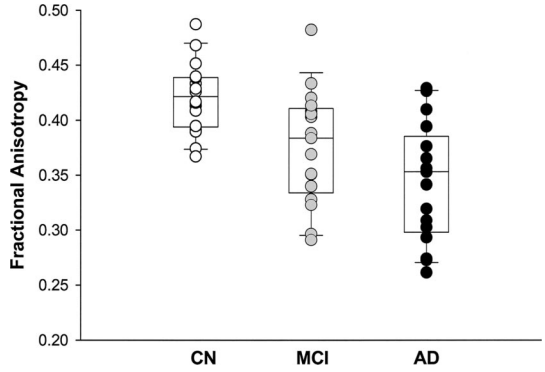

Figure 3. Scatter and box plots of fractional anisotropy in the left posterior cingulate in cognitive normal (○, mean ± SD = 0.42 ± 0.03), mild cognitive impairment (◍ , 0.38 ± 0.05), and Alzheimer disease (●, 0.34 ± 0.05).

CN ($p < 0.0001$) or MCI ($p < 0.0001$), and further, MCI subjects had lower MMSE scores than CN ($p = 0.02$). CDR scores for each group are listed as well.

Fractional anisotropy. Results from modeling FA as a function of diagnosis are summarized in table 2, separately for each ROI region. Compared to CN, patients with AD had lower FA values bilaterally in both parahippocampal (left $p = 0.002$; right $p = 0.04$) and posterior cingulate regions (left $p < 0.0001$; right $p = 0.003$). Moreover, patients with AD had markedly lower FA values in the splenium ($p = 0.003$) than CN subjects, while the genu was spared ($p = 0.39$) in AD. Similar to AD, patients with MCI—when compared to CN—had lower FA values bilaterally in parahippocampal regions (left $p = 0.01$; right $p = 0.02$), and in the left posterior cingulate ($p = 0.003$). However, MCI showed no change in the splenium ($p = 0.11$) and the genu ($p = 0.6$). Comparing AD to MCI showed that the two groups had similar FA reductions in parahippocampal regions (left $p = 0.69$; right $p = 0.79$) and in the left posterior cingulate ($p = 0.12$), while patients with MCI had less FA reductions than AD in the right posterior cingulate ($p = 0.004$) and the splenium ($p = 0.01$). Finally, CN, MCI, and AD had similar FA values in the internal capsule ($p > 0.05$), as expected. FA reductions in the left posterior cingulate yielded the largest effect size between CN subjects and MCI (effect size = –1.07) or AD (effect size = –1.76). The scatter plot in figure 3 depicts the distribution of FA values of the left posterior cingulate, separately for CN, MCI, and AD subjects. Notably, FA differences between the groups remained significant after accounting for age. In addition, adding years of education into the model did not alter the significance of FA differences between the groups.

Diffusivity. Results for D as a function of diagnosis are summarized in table 3. Compared to CN subjects, patients with AD had increased D values bilaterally in parahippocampal (left $p = 0.03$; right $p = 0.002$) and posterior cingulate regions (left $p = 0.01$; right $p = 0.01$), while patients with MCI had slightly increased D values only in left posterior cingulate regions ($p = 0.04$). Compared to MCI, patients with AD had increased D values in the right posterior cingulate ($p = 0.01$). Similar to FA, differences in D between groups remained significant after accounting for age and years of education. Furthermore, no differences in D ($p > 0.05$) were found across groups in bilateral internal capsule and the genu.

Table 3 *Group effects of diagnosis on diffusivity*

Dependent variable	Coefficients value	SE	*p* Value	Effect size
AD vs CN				
Left PH	0.22	0.09	0.03	0.78
Right PH	0.39	0.12	0.002	1.25
Left PC	0.24	0.09	0.01	0.95
Right PC	0.24	0.09	0.01	1.04
sCC	0.18	0.17	0.31	0.44
gCC	0.11	0.16	0.5	0.45
MCI vs CN				
Left PH	0.1	0.09	0.28	0.4
Right PH	0.17	0.09	0.06	0.73
Left PC	0.16	0.08	0.04	0.82
Right PC	−0.04	0.07	0.59	−0.08
sCC	−0.07	0.12	0.53	−0.15
gCC	−0.21	0.13	0.13	−0.35
AD vs MCI				
Left PH	0.1	0.1	0.34	0.41
Right PH	0.21	0.12	0.1	0.58
Left PC	0.06	0.1	0.55	0.21
Right PC	0.23	0.09	0.01	1.06
sCC	0.21	0.17	0.23	0.55
gCC	0.27	0.16	0.1	0.77

AD = Alzheimer disease; CN = cognitive normal; PH = parahippocampus; PC = posterior cingulate; sCC = splenium and gCC = genu of the corpus callosum; MCI = mild cognitive impairment.

Hippocampal volume. The scatter plot in figure 4 depicts the distributions of left hippocampal volumes, separately in CN, MCI, and AD. Comparing MCI to CN, hippocampal volumes were smaller only on the right side ($p = 0.03$) but not on the left side ($p = 0.16$), while age made contributions to the volume differences between MCI and CN on both sides (left $p = 0.001$, right $p = 0.002$). For

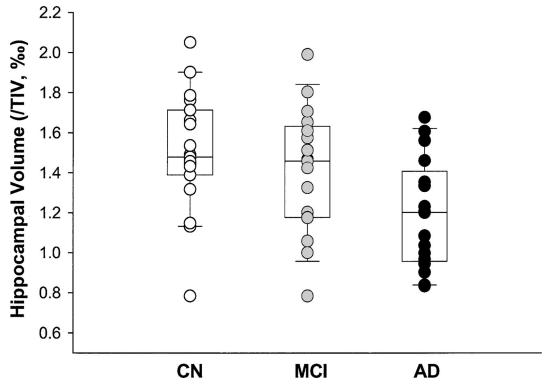

Figure 4. Scatter and box plots of the left hippocampal volume (in thousandth of total intracranial volume) in cognitive normal (○, mean ± SD = 1.5 ± 0.2), mild cognitive impairment (◍ , 1.4 ± 0.3), and Alzheimer disease (●, 1.2 ± 0.3).

Copyright © by AAN Enterprises, Inc. Unauthorized reproduction of this article is prohibited.

Table 4 *Group effects on hippocampal volumes, accounting for age*

Dependent variable	Independent variables	Coefficient	SE	*p* Value	Effect size
MCI vs CN					
Left HV	Age	−257	70	0.001	N/A
	Dx	−774	541	0.16	0.5
Right HV	Age	−241	70	0.002	N/A
	Dx	−1,225	536	0.03	0.76
AD vs CN					
Left HV	Age	−110	65	0.1	N/A
	Dx	−2,226	588	<0.001	−1.38
Right HV	Age	−87	72	0.23	N/A
	Dx	−2,094	651	0.003	−1.35
AD vs MCI					
Left HV	Age	−101	93	0.29	N/A
	Dx	−1,506	695	0.04	−0.74
Right HV	Age	−125	112	0.27	N/A
	Dx	−748	837	0.38	−0.45

MCI = mild cognitive impairment; CN = cognitive normal; AD = Alzheimer disease; HV = hippocampal volume; Dx = diagnosis; N/A = not available.

patients with AD, however, smaller hippocampal volumes compared to CN were entirely explained by diagnosis (left $p < 0.001$; right $p = 0.003$) while age made no contribution ($p \geq 0.1$) (see also table 4). Finally, compared to MCI, patients with AD had smaller hippocampal volumes on the left side ($p = 0.04$), but not on the right side ($p = 0.38$), while age made no significant contributions. Similar to DTI measures, years of education did not make any significant contribution to hippocampal volume differences across groups.

Classifications. Since the FA reduction in the left posterior cingulate yielded the largest effect size between CN and MCI or AD, this measure was used to compare the powers of DTI and hippocampal volumes to correctly classify MCI, AD, and CN subjects. Results from a logistic regression analysis and a receiver operator characteristics analysis are summarized in table 5.

Hippocampal volume alone could not reliably separate MCI from CN subjects ($p = 0.1$), yielding no more than 63 ± 3% (mean ± SD) accuracy, 55 ± 8% sensitivity, and 70 ± 5% specificity with an area under the receiver operator characteristics curve (AUC) of 0.67 ± 0.02. The addition of FA improved classification ($p = 0.02$), increasing accuracy to 74 ± 2%, sensitivity to 69 ± 3%, and specificity to 78 ± 2% with an increased ($p < 0.001$) AUC of 0.78 ± 0.02. Hippocampal volume alone, however, separated AD from CN subjects reliably ($p = 0.007$), yielding 78 ± 1% accuracy, 75 ± 3% sensitivity, and 81 ± 3% specificity with an AUC of 0.85 ± 0.01. The addition of FA improved the classification further ($p < 0.001$), resulting in 91 ± 1% accuracy and 88 ± 1% for sensitivity and 94 ± 2% for specificity. The AUC also increased ($p < 0.001$), reaching a value of 0.98 ± 0.002, which indicates almost complete separation of the groups.

Discussion. We found that 1) MCI is associated with FA reductions particularly in the cingulum fibers, predominantly in the left posterior cingulate. In AD, FA is further reduced in the cingulum fibers and FA reductions extend to the splenium, consistent with previous reports. 2) FA reductions in the posterior cingulate improved the classification of MCI and AD from cognitively normal elderly compared to the classifications using hippocampal volume loss alone.

To explain the dissociation between PET/SPECT and MRI findings in MCI and AD, we hypothesized that the integrity of the cingulum fibers, which connect the posterior cingulate gyrus and the hippocampus,[13,14] may be compromised in the early stage of AD. Although the exact nature of the fiber disintegration is unclear, FA reduction, coupled with increased diffusivity, is thought to reflect axonal loss or demyelination.[37,38] Our finding of prominent FA reduction in posterior cingulate regions in MCI is consistent with previous reports,[21,22] and the substantial FA reductions in parahippocampal regions in MCI further establishes the vulnerability of the cingulum fibers in the early stage of AD. Taken together, these findings support our hypothesis that the entire connections between hippocampus and posterior cingulate are affected in the early stage of AD. Furthermore, we found that the FA values of the cingulum fibers in MCI are significantly lower

Table 5 *Group classifications by hippocampal volume and fractional anisotropy of posterior cingulate*

Classification	Factors	Sensitivity (%)	Specificity (%)	Accuracy (%)	*p* Value*	AUC	*p* Value†
MCI vs CN	Total HV	55 ± 8	70 ± 5	63 ± 3	0.1	0.67 ± 0.02	
	TotalHV+LeftPC-FA	69 ± 3	78 ± 2	74 ± 2	0.02	0.78 ± 0.02	<0.001
AD vs CN	Total HV	75 ± 3	81 ± 3	78 ± 1	0.007	0.85 ± 0.01	
	TotalHV+LeftPC-FA	88 ± 1	94 ± 2	91 ± 1	<0.001	0.98 ± 0.002	<0.001

* From logistic regression.
† From a Wilcoxon signed rank test, comparing two areas under the curves (AUC).

MCI = mild cognitive impairment; CN = cognitive normal; HV = hippocampal volume; left PC-FA = FA of the left posterior cingulate; AD = Alzheimer disease.

Copyright © by AAN Enterprises, Inc. Unauthorized reproduction of this article is prohibited.

than in controls but very close to the FA values in AD group, whereas the hippocampal volumes in MCI are intermediate between AD and control and in fact not significantly different from control. If we conceptualize MCI as representing early AD, our findings suggest that DTI measures of FA in the cingulum fibers may be a more sensitive marker of early AD pathology than hippocampal volume. Therefore, if these findings are replicated, DTI measures of FA in the cingulum fibers may be used as an early predictor of future cognitive decline and development of AD.

Consistent with previous DTI studies in AD, we also found FA reductions in posterior aspects but not anterior aspects of the CC.[22,25] Anatomically, the posterior CC connects the temporal and parietal cortices, while the anterior CC connects frontal cortices.[39] Thus, our finding supports the suggestion that the temporoparietal connections are more impacted than frontal connections by AD.

We also found that FA reductions of cingulum fibers, especially in the left posterior cingulate region, improved the classification between MCI and elderly controls over using hippocampal volume alone. Hippocampal volume could not accomplish reliable classification between MCI and CN, independent of whether adjustments for age effects were made. Moreover, FA of the cingulum fibers significantly improved the separation of AD from control subjects, achieving almost complete separation between the groups, compared to an already high classification power using hippocampal volume alone. Taken together, the results suggest that measuring the FA value in the cingulum fibers could be a supplementary marker to the hippocampal volume in diagnoses of MCI and AD. Prospective studies are underway to determine if DTI predicts cognitive decline and conversion to AD.

Our study has several limitations. Since we did not follow patients with MCI longitudinally to determine conversion to AD, it remains to be seen whether the DTI findings in MCI were related to AD or indicates perhaps other types of dementia. Another limitation is that DTI observations in AD and MCI could be related to other factors than the AD pathology, such as WML due to cerebral vascular disease, although the groups were matched by WML severity and the subjects with WML involving the ROI were not included in this study. The relation between fiber integrity and cerebral vascular disease needs to be further explored. Lastly, it cannot be excluded that inclusion of CSF, as a consequence of brain atrophy, may have biased DTI results in AD and MCI toward lower FA and higher D values, despite our attempts to suppress the CSF signal by using an inversion-recovery DTI sequence. Therefore, our DTI results may not entirely be decoupled from underlying brain atrophy and more work needs to be done to develop techniques that further reduce or eliminate this confound from DTI measurements.

Acknowledgment

The authors thank Dr. John Kornak for advice in statistics and Drs. Xiaoping Zhu and Kaloh Li for help with logistic regression scripts. They also thank Mrs. Diana Truran-Sacrey, Ms. Erin Clevenger, and Ms. Dawn Hardin for measuring hippocampal volumes and image processing.

References

1. Du AT, Schuff N, Amend D, et al. Magnetic resonance imaging of the entorhinal cortex and hippocampus in mild cognitive impairment and Alzheimer's disease. J Neurol Neurosurg Psychiatry 2001;71:441–447.
2. Jack CR Jr., Petersen RC, Xu YC, et al. Prediction of AD with MRI-based hippocampal volume in mild cognitive impairment. Neurology 1999;52:1397–1403.
3. Petersen RC, Smith GE, Tangalos EG, et al. Clinical course of patients with a mild cognitive impairment. Neurology 1993;43:(A277).
4. Killiany RJ, Gomez-Isla T, Moss M, et al. Use of structural magnetic resonance imaging to predict who will get Alzheimer's disease. Ann Neurol 2000;47:430–439.
5. Du AT, Schuff N, Laakso MP, et al. Effects of subcortical ischemic vascular dementia and AD on entorhinal cortex and hippocampus. Neurology 2002;58:1635–1641.
6. Xu Y, Jack CJ, O'Brien PC, et al. Usefulness of MRI measures of entorhinal cortex versus hippocampus in AD. Neurology 2000;54:1760–1767.
7. Minoshima S, Frey KA, Koeppe RA, et al. A diagnostic approach in Alzheimer's disease using three- dimensional stereotactic surface projections of fluorine-18-FDG PET. J Nucl Med 1995;36:1238–1248.
8. Mielke R, Kessler J, Szelies B, et al. Normal and pathological aging–findings of positron-emission-tomography. J Neural Transm 1998;105:821–837.
9. Jagust WJ. Neuroimaging in dementia. Neurol Clin 2000;18:885–902.
10. Petrella JR, Coleman RE, Doraiswamy PM. Neuroimaging and early diagnosis of Alzheimer disease: a look to the future. Radiology 2003;226:315–336.
11. Arnaiz E, Jelic V, Almkvist O, et al. Impaired cerebral glucose metabolism and cognitive functioning predict deterioration in mild cognitive impairment. Neuroreport 2001;12:851–855.
12. Chetelat G, Desgranges B, de la Sayette V, et al. Mild cognitive impairment: can FDG-PET predict who is to rapidly convert to Alzheimer's disease? Neurology 2003;60:1374–1377.
13. Wakana S, Jiang H, Nagae-Poetscher LM, et al. Fiber tract-based atlas of human white matter anatomy. Radiology 2004;230:77–87.
14. Catani M, Howard RJ, Pajevic S, et al. Virtual in vivo interactive dissection of white matter fasciculi in the human brain. Neuroimage 2002;17:77–94.
15. Braak E, Griffing K, Arai K, et al. Neuropathology of Alzheimer's disease: what is new since A. Alzheimer? Eur Arch Psychiatry Clin Neurosci 1999; 249 suppl 3:14–22.
16. Beaulieu C, Does MD, Snyder RE, et al. Changes in water diffusion due to Wallerian degeneration in peripheral nerve. Magn Reson Med 1996;36:627–631.
17. Suzuki Y, Matsuzawa H, Kwee IL, et al. Absolute eigenvalue diffusion tensor analysis for human brain maturation. NMR Biomed 2003;16:257–260.
18. Schneider JF, Il'yasov KA, Boltshauser E, et al. Diffusion tensor imaging in cases of adrenoleukodystrophy: preliminary experience as a marker for early demyelination? AJNR Am J Neuroradiol 2003;24:819–824.
19. Le Bihan D, Mangin JF, Poupon C, et al. Diffusion tensor imaging: concepts and applications. J Magn Reson Imaging 2001;13:534–546.
20. Yoshiura T, Mihara F, Ogomori K, et al. Diffusion tensor in posterior cingulate gyrus: correlation with cognitive decline in Alzheimer's disease. Neuroreport 2002;13:2299–2302.
21. Fellgiebel A, Muller MJ, Wille P, et al. Color-coded diffusion-tensor-imaging of posterior cingulate fiber tracts in mild cognitive impairment. Neurobiol Aging 2005;26:1193–1198.
22. Takahashi S, Yonezawa H, Takahashi J, et al. Selective reduction of diffusion anisotropy in white matter of Alzheimer disease brains measured by 3.0 Tesla magnetic resonance imaging. Neurosci Lett 2002;332:45–48.
23. Fellgiebel A, Wille P, Muller MJ, et al. Ultrastructural hippocampal and white matter alterations in mild cognitive impairment: a diffusion tensor imaging study. Dement Geriatr Cogn Disord 2004;18:101–108.
24. Bozzali M, Falini A, Franceschi M, et al. White matter damage in Alzheimer's disease assessed in vivo using diffusion tensor magnetic resonance imaging. J Neurol Neurosurg Psychiatry 2002;72:742–746.
25. Rose SE, Chen F, Chalk JB, et al. Loss of connectivity in Alzheimer's disease: an evaluation of white matter tract integrity with colour coded MR diffusion tensor imaging. J Neurol Neurosurg Psychiatry 2000;69:528–530.

Copyright © by AAN Enterprises, Inc. Unauthorized reproduction of this article is prohibited.

26. Stahl R, Dietrich O, Teipel S, et al. [Assessment of axonal degeneration on Alzheimer's disease with diffusion tensor MRI.] Radiologe 2003;43: 566–575.
27. Head D, Buckner RL, Shimony JS, et al. Differential vulnerability of anterior white matter in nondemented aging with minimal acceleration in dementia of the Alzheimer type: evidence from diffusion tensor imaging. Cereb Cortex 2004;14:410–423.
28. Folstein MF, Folstein SE, McHugh PR. "Mini-mental state". A practical method for grading the cognitive state of patients for the clinician. J Psychiatr Res 1975;12:189–198.
29. Morris JC. The Clinical Dementia Rating (CDR): current version and scoring rules. Neurology 1993;43:2412–2414.
30. Petersen RC, Smith GE, Waring SC, et al. Mild cognitive impairment: clinical characterization and outcome. Arch Neurol 1999;56: 303–308.
31. Mohs RC, Knopman D, Petersen RC, et al. Development of cognitive instruments for use in clinical trials of antidementia drugs: additions to the Alzheimer's Disease Assessment Scale that broaden its scope. The Alzheimer's Disease Cooperative Study. Alzheimer Dis Assoc Disord 1997; 11 suppl 2:S13–S21.
32. McKhann G, Drachman D, Folstein M, et al. Clinical diagnosis of Alzheimer's disease: report of the NINCDS- ADRDA Work Group under the auspices of Department of Health and Human Services Task Force on Alzheimer's Disease. Neurology 1984;34:939–944.
33. Scheltens P, Barkhof F, Leys D, et al. Semiquantitative rating scale for the assessment of signal hyperintensities on magnetic resonance imaging. J Neurol Sci 1993;114:7–12.
34. Reese TG, Heid O, Weisskoff RM, et al. Reduction of eddy-current-induced distortion in diffusion MRI using a twice-refocused spin echo. Magn Reson Med 2003;49:177–182.
35. Hsu YY, Schuff N, Du AT, et al. Comparison of automated and manual MRI volumetry of hippocampus in normal aging and dementia. J Magn Reson Imaging 2002;16:305–310.
36. Jiang H, van Zijl PC, Kim J, et al. DtiStudio: resource program for diffusion tensor computation and fiber bundle tracking. Comput Methods Programs Biomed 2006;81:106–116.
37. Basser PJ, Pierpaoli C. Microstructural and physiological features of tissues elucidated by quantitative-diffusion-tensor MRI. J Magn Reson B 1996;111:209–219.
38. Sullivan EV, Pfefferbaum A. Diffusion tensor imaging in normal aging and neuropsychiatric disorders. Eur J Radiol 2003;45: 244–255.
39. Huang H, Zhang J, Jiang H, et al. DTI tractography based parcellation of white matter: application to the mid-sagittal morphology of corpus callosum. Neuroimage 2005;26:195–205.

Neuro*Images*

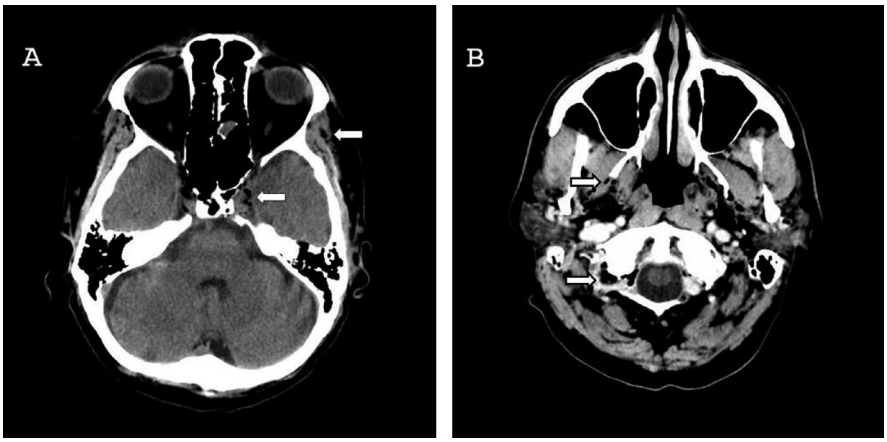

Figure. Extracranial venous air embolism: first arrow from the top in A and white arrows in B. Cavernous sinus gas embolism: second arrow from the top in A.

Headache and cerebral venous air embolism

Stephan A. Botez, MD, Lausanne, Switzerland

A 47-year-old man with migraine without aura presented with bilateral throbbing sudden onset headache resistant to usual triptan medication. He had dental implants revised 3 days earlier. General and neurologic examinations were normal. Brain CT showed cerebral venous gas embolism (figure). The headache resolved with 100% oxygen therapy in flat supine position. Brain CT was normal 48 hours later. Cerebral venous air embolism was probably secondary to an aberrant communication between air and venous system during dental surgery resulting in retrograde cerebral venous air embolism,[1] an underestimated diagnosis because it is often clinically silent.[2]

Copyright © 2007 by AAN Enterprises, Inc.

Disclosure: The author reports no conflicts of interest.

Address correspondence and reprint requests to Dr. Botez, Neurology Department, Centre Hospitalier Universitaire Vaudois (CHUV), Rue du Bugnon 46, 1011-Lausanne, Switzerland; e-mail: Stephan.Botez@chuv.ch

1. Schlimp CJ, Loimer T, Rieger M, Lederer W, Schmidts MB. The potential of venous air embolism ascending retrograde to the brain. J Forensic Sci 2005;50:906–909.
2. Rubinstein D, Dangleis K, Damiano TR. Venous air emboli identified on head and neck CT scans. J Comput Assist Tomogr 1996;20:559–562.

Copyright © by AAN Enterprises, Inc. Unauthorized reproduction of this article is prohibited.

Neurology®

Headache and cerebral venous air embolism

Stephan A. Botez

Neurology 2007;68;19
DOI 10.1212/01.wnl.0000236902.50380.ba

This information is current as of January 2, 2007

Updated Information & Services	including high resolution figures, can be found at: http://www.neurology.org/content/68/1/19.full.html
Supplementary Material	Supplementary material can be found at: http://www.neurology.org/content/suppl/2007/06/11/68.1.19.DC1.html
References	This article cites 2 articles, 0 of which you can access for free at: http://www.neurology.org/content/68/1/19.full.html##ref-list-1
Citations	This article has been cited by 2 HighWire-hosted articles: http://www.neurology.org/content/68/1/19.full.html##otherarticles
Subspecialty Collections	This article, along with others on similar topics, appears in the following collection(s): **All Cerebrovascular disease/Stroke** http://www.neurology.org//cgi/collection/all_cerebrovascular_disease_stroke **MRI** http://www.neurology.org//cgi/collection/mri
Permissions & Licensing	Information about reproducing this article in parts (figures,tables) or in its entirety can be found online at: http://www.neurology.org/misc/about.xhtml#permissions
Reprints	Information about ordering reprints can be found online: http://www.neurology.org/misc/addir.xhtml#reprintsus

Neurology ® is the official journal of the American Academy of Neurology. Published continuously since 1951, it is now a weekly with 48 issues per year. Copyright . All rights reserved. Print ISSN: 0028-3878. Online ISSN: 1526-632X.

AMERICAN ACADEMY OF NEUROLOGY®